Multiscale simulations in face-centered cubic metals: A method coupling quantum mechanics and molecular mechanics *

Yu Xiao-Xiang(于潇翔)[a)b)†] and Wang Chong-Yu(王崇愚)[b)]

[a)] *Department of Materials Science and Engineering, Tsinghua University, Beijing* 100084, *China*
[b)] *Department of Physics, Tsinghua University, Beijing* 100084, *China*

(Received 1 September 2012; revised manuscript received 25 September 2012)

An effective multiscale simulation which concurrently couples the quantum-mechanical and molecular-mechanical calculations based on the position continuity of atoms is presented. By an iterative procedure, the structure of the dislocation core in face-centered cubic metal is obtained by first-principles calculation and the long-range stress is released by molecular dynamics relaxation. Compared to earlier multiscale methods, the present work couples the long-range strain to the local displacements of the dislocation core in a simpler way with the same accuracy.

Keywords: first-principles calculation， molecular dynamics， dislocation structure

PACS: 71.15.Mb，71.15.Pd，61.72.Lk **DOI:** 10.1088/1674-1056/22/2/027101

1. Introduction

Initiation, motion, and evolution of dislocations play an important role in the plastic deformation and mechanical properties of materials. Many dynamic processes such as dislocation climb, cross-slip, and diffusion of atoms depend on the atomic structure of the dislocation core. Accurate modeling of the dislocation core configuration is the key to understanding the mechanism of dislocation movement and the interaction between solid-solution elements and dislocation in alloys. Elastic theory can deal with far-field distributions of stress and strain for dislocation but the elastic solution diverges near the dislocation core. Molecular dynamics (MD) is a powerful tool to simulate structural evolution at the atomic level but the accuracy of the result largely depends on the interatomic potential used in the simulation. Moreover, the empirical potentials are limited by their capability to provide details regarding the chemical contributions of solid-solution elements. Density functional theory (DFT) can provide accurate calculations on the electronic and atomic structures of local defects in materials but the long-range strain field produced by a dislocation is too large to be studied directly by DFT. Several multiscale methods have been developed to couple DFT calculation with elastic theory or MD simulation. For example, based on the framework of the Peierls–Nabarro model, the core structures and properties of dislocations in some materials[1–8] have been studied by combining DFT with elastic theory using the concept of generalized-stacking fault (GSF) energy introduced by Vitek.[9,10] This method needs the nonlinear misfit energy obtained by GSF energy derived from first-principles calculations and the elastic energy calculated in the continuum framework. Therefore the accuracy of the method relies on the reliability of both GSF energy and the elastic energy of the dislocation. Choly *et al.*[11] coupled DFT-based calculations with empirical embedded-atom-method (EAM) simulations for simple metals. They divided the system into two subsystems: quantum-mechanical (QM) region where detailed physics were relevant and the rest of the system was molecular-mechanical (MM) region. The total energy of the system was the sum of the energy of QM region evaluated with DFT, the energy of MM region calculated via a classical potential and the interaction energy between the two subsystems which can be treated using both classical potential and quantum-mechanical method. The total energy of the system was minimized with respect to the coordinates of atoms in an iterative way until the system was relaxed. Lu *et al.*[12,13] improved upon Choly's method and developed a quasicontinuum DFT (QCDFT) method which concurrently couples DFT calculation to MD simulation and to finite-element modeling in a unified description for metallic systems. The efficiency of this coupling scheme has been demonstrated in an aluminum system.[14,15] Woodward *et al.*[16–20] developed the first-principles lattice Green function boundary condition method (FP-GFBC) to couple the local dislocation strain field to the long-range elastic field using a flexible boundary condition. In the FP-GFBC method, the incompatibility forces produced by the DFT region were relaxed by moving all the atoms in the simulation cell according to the Greens function solution. This method has been applied to dislocations in bcc molybdenum and tantalum metals, fcc iridium and aluminum metals, and ordered alloys. QCDFT and FP-GFBC are effective methods to predict and simulate the core structure of dislocation, but complicated processes exist during the simulations in both methods. For the QCDFT method, in order to couple

*Project supported by the National Basic Research Program of the Ministry of Science and Technology of China (Grant No. 2011CB606402) and the National Natural Science Foundation of China (Grant No. 51071091).

†Corresponding author. E-mail: yuxx07@gmail.com

© 2013 Chinese Physical Society and IOP Publishing Ltd

QM and MM regions, the interaction energy between these two regions must be calculated. Treating the interaction energy using different methods will induce different results. For the FP-GFBC method, the lattice Green function for a given crystal structure must be derived using the calculated elastic constants and the force-constant matrix, which increases the complexity of the simulations. In addition, the result of the simulation relies on the accuracy of the Green function's solution.

In this paper, we perform a simple and effective QM and MM coupling simulation to study the core structures of dislocations. Our method is based on the position continuity of atoms across different scales. The positions of atoms in one region and another mutually act as the boundary condition for each other. In the simulation, the system is divided into three regions: MM region, coupling region, and QM region. The method proceeds as follows: (i) the initial positions of atoms are approximated by the anisotropic elastic solution of the dislocation. (ii) The positions of atoms within the QM region are optimized using a DFT method. The atoms within the coupling region are fixed as the boundary conditions of the QM region during the relaxation. (iii) The atoms in the coupling region and the MM region are relaxed by a MD method holding the atoms in the QM region fixed to relieve the incompatible forces for the atoms in the coupling region. Steps (ii) and (iii) are repeated until the force and displacement are sufficiently small. By the iterative procedure, the structure of the dislocation core can be obtained accurately by DFT calculation and the long-range stress can be released by MD relaxation. To check the validity of our method, we first study the dislocation in aluminum because many experimental and calculated results are available for comparison. Also we demonstrate the effectiveness and transferability of this approach by studying edge and screw dislocations in nickel. The details of our calculations and results are discussed below.

2. Computational models and methods

The relaxations of edge dislocations are calculated in the cells of 137.5 Å×140.3 Å×4.96 Å (1 Å = 0.1 nm) for Al and 119.5 Å×121.9 Å×4.31 Å for Ni in the x[110], y[1$\bar{1}$1], and z[1-1-2] directions as shown in Fig. 1(a). The dashed box represents the QM region. The two layers of atoms around the QM region are the coupling-region atoms. In step (i), an edge dislocation is introduced in the center of the cell by the anisotropic elastic solution. In step (ii), all the atoms in both QM and coupling regions are calculated by the DFT method while the positions of the coupling-region atoms are fixed, and a 15-Å vacuum region outside the coupling region is introduced in x and y directions to separate the dislocation from its periodic images. The vacuum region will produce a charge dipole at the surface with decaying Friedel oscillations in the charge density.[16,19] In order to isolate the dislocation core electrostatically from the surface, the cell size of QM region needs to be big enough. For the calculation of Al, the QM region contains 136 atoms surrounded by 116 atoms in the coupling region. For the calculation of Ni, the QM region contains 184 atoms surrounded by 140 atoms in the coupling region. The DFT calculations are carried out with the plane-wave based Vienna *ab initio* simulation package (VASP) [21,22] using the projector augmented wave method [23,24] and the generalized gradient approximation in the parameterization, as developed by Perdew *et al*.[25] Plane waves have been included up to a cutoff energy of 360 eV for both Al and Ni, which yields converged results. The convergence accuracy of total energy is chosen as 10^{-5} eV in the relaxation of electronic degrees of freedom. The structures of the models are relaxed until the maximum force is less than 0.02 eV/Å. The scheme of k points sampling is set up according to the Monkhorst–Pack scheme.[26]

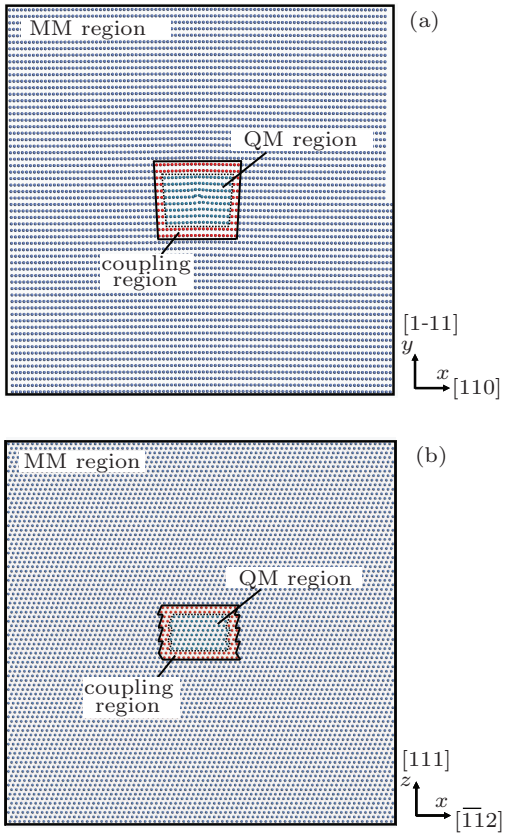


Fig. 1. (color online) The computational cells of edge and screw dislocations. (a) Model for an edge dislocation containing 5760 atoms in total. (b) Model for a screw dislocation containing 6720 atoms in total.

In step (iii), the positions of atoms in the QM region are updated by the results of step (ii), and the positions of atoms in the coupling and MM regions are optimized by MD calculation, while the atoms in the QM region are fixed. The MD relaxations are carried out using the EAM potentials of Al and Ni developed by Mishin *et al*.[27] The properties of Al and Ni predicted by Mishin potentials agree well with those

from experimental and *ab initio* data. Fixed boundary conditions are applied along the x and y directions and periodic boundary conditions are applied along the z direction to simulate a straight dislocation. Steps (ii) and (iii) iterate until the maximum force is less than 0.02 eV/Å in both the coupling region and the QM region.

The relaxations of screw dislocations are calculated in the cells of 198.4 Å×2.87 Å×196.4 Å for Al and 172.4 Å×2.49 Å×170.7 Å for Ni in the $x[\bar{1}\,\bar{1}2]$, $y[1\bar{1}0]$, and $z[111]$ directions as shown in Fig. 1(b). For both Al and Ni, the QM region contains 96 atoms surrounded by 96 atoms in the coupling region. The procedure of simulation is the same as that of the edge dislocation mentioned above. In step (ii), the 192 atoms in the QM and coupling regions are calculated using VASP while 96 coupling-region atoms are fixed and a 15-Å vacuum region is introduced in the x and z directions. During the MD relaxation in step (iii), fixed boundary conditions are applied along the x and z directions and periodic boundary conditions are applied along the y direction. The convergence criterion of force is also less than 0.02 eV/Å in both the coupling region and the QM region.

3. Computational results and discussion

Figures 2(a) and 3(a) show the maximum forces on the coupling-region Al atoms given by EAM potential after DFT calculation in step (ii) and before MD relaxation in step (iii) in each iteration for edge and screw dislocations respectively. Since the relaxation by DFT has been finished in step (ii), the maximum force in the QM region is less than 0.02 eV/Å. However, the forces on the coupling-region atoms are not released because they are fixed during the DFT relaxation. The MD relaxation in step (iii) will release the forces in the coupling region but change the boundary condition of the QM region. As the iterations go on, the maximum force in the coupling region before the MD relaxation step decreases. For edge dislocation, after 8 iterations, the maximum force in the QM region is less than 0.02 eV/Å after step (ii) and the maximum force in the coupling region is also less than 0.02 eV/Å before step (iii). Although the forces in the QM region and the coupling region are calculated by different methods, they decrease to the convergence criteria of force respectively, which means the incompatibility forces between the QM and MM regions are released. For screw dislocation, the convergence criterion of force is achieved after 6 iterations.

Figures 2(b) and 3(b) show the maximum displacements of coupling-region atoms between the current and previous iterations after MD relaxations for edge and screw dislocations, respectively. The results show the displacements decrease as the iterations continue, which means the displacements are converging in coupling regions.

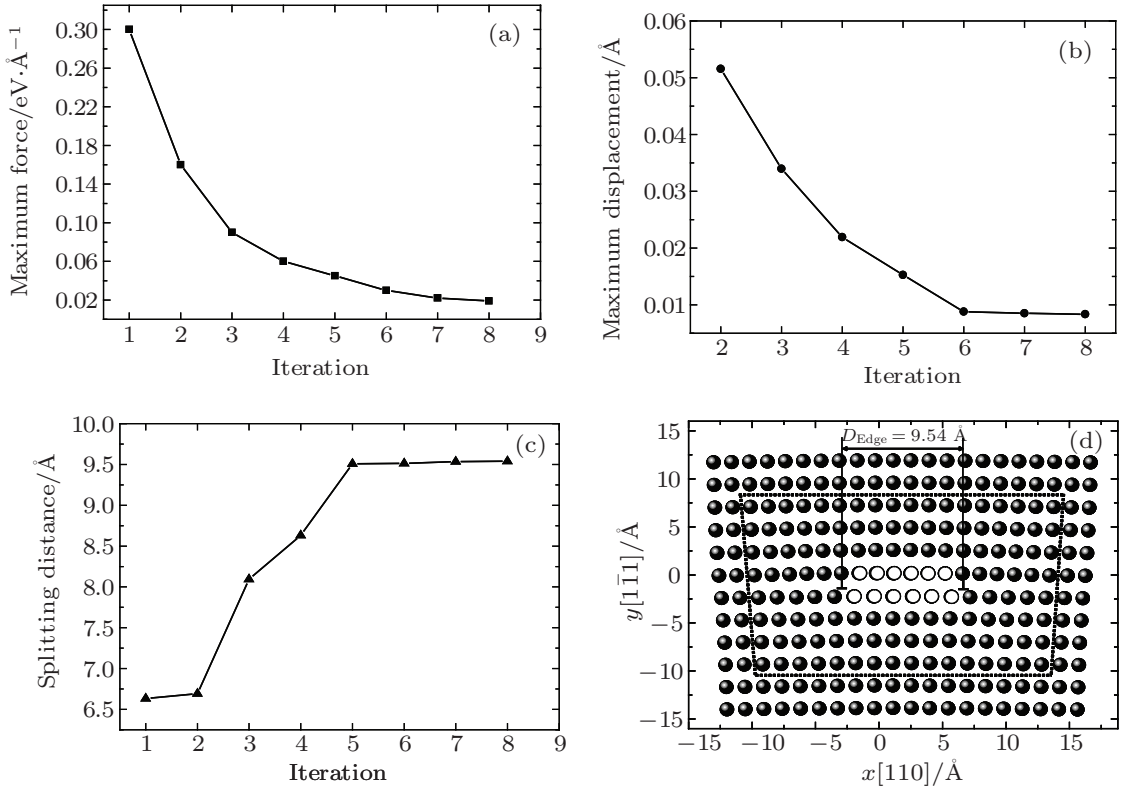


Fig. 2. The computational results for an edge dislocation in Al. (a) The maximum force on the coupling-region Al atoms before MD relaxation in each iteration. (b) The maximum displacement of the coupling-region Al atoms between two consecutive iterations. (c) The splitting distance between two partial dislocations in each iteration. (d) The core structure of the dissociated edge dislocation in Al. The open circles represent the atoms with HCP structures and the full circles represent the atoms with FCC structures. The dashed box represents the QM region. The atoms around the QM region are the coupling-region atoms.

A perfect dislocation will dissociate into two partial dislocations in FCC metal separated by a stacking fault. The stacking fault corresponds to a block with HCP structure inserted in the FCC structure. We perform a common neighbor analysis (CNA)[28] implemented in OVITO software[29] to identify the HCP structure in FCC matrix and determine the splitting distance between two partial dislocations. In this analysis, each atom in the system is assigned a structural type (FCC, BCC, HCP etc.) based on a nearest-neighbor graph which describes the connectivity among neighbors of a given central atom. From the width of the HCP structure, the splitting distance between two partial dislocations can be obtained. The changes of the splitting distances as the iterations go on are shown in Figs. 2(c) and 3(c). The convergent splitting distances of edge and screw dislocations in Al are 9.54 Å and 7.53 Å. The atomic core structures of edge and screw dislocations are shown in Figs. 2(d) and 3(d). The open circles represent the atoms with HCP structures and the full circles represent the atoms with FCC structures. The dashed box represents the QM region. The atoms around the QM region are the coupling-region atoms. Table 1 lists the experimental and calculated separation distances for Al edge and screw partial dislocations in previous studies.[2,4,12–15,19,20,30] Compared to the first-principles GSF, QCDFT, and FP-GFBC methods, our results are close to the values obtained by FP-GFBC method.

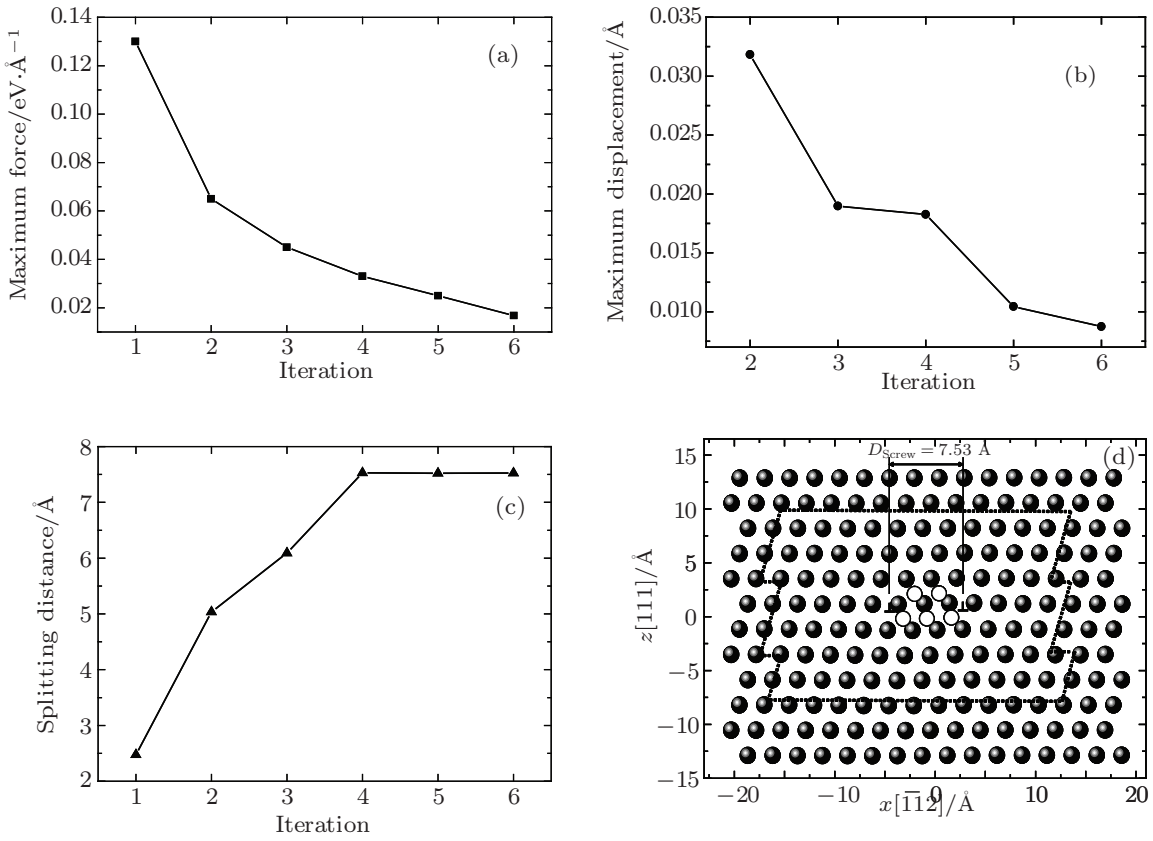


Fig. 3. The computational results for a screw dislocation in Al. (a) The maximum force on the coupling-region Al atoms before MD relaxation in each iteration. (b) The maximum displacement of the coupling-region Al atoms between two consecutive iterations. (c) The splitting distance between two partial dislocations in each iteration. (d) The core structure of the dissociated screw dislocation in Al.

Table 1. The partial splitting distances for $a/2\langle 110\rangle$ edge and screw dislocations in Al.

Method	edge/Å	Screw/Å
Present work	9.54	7.53
FP-GSF	7.4[a], 3.5[b]	2.1[b]
QCDFT	5.6[c], 5.9[d], 7.0[e]	–
FP-GFBC	7.0∼9.5[f], 10.8[g]	5.0∼7.5[f]
Experiment	8.0[h]	–

[a]Ref. [2], [b]Ref. [4], [c]Ref. [12], [d]Ref. [13], [e]Ref. [14], [15], [f]Ref. [19], [g]Ref. [20], [h]Ref. [30]

For edge and screw dislocations in Ni, figures 4(a) and 4(c) show the maximum forces of Ni atoms within the coupling region converge after 16 and 12 iterations. The convergent splitting distance of edge dislocation in Ni is 15.66 Å which is close to the lower limit of experimental results in Table 2.[31] The convergent splitting distance of screw dislocation is 8.63 Å. The atomic core structures of edge and screw dislocations are shown in Figs. 4(b) and 4(d).

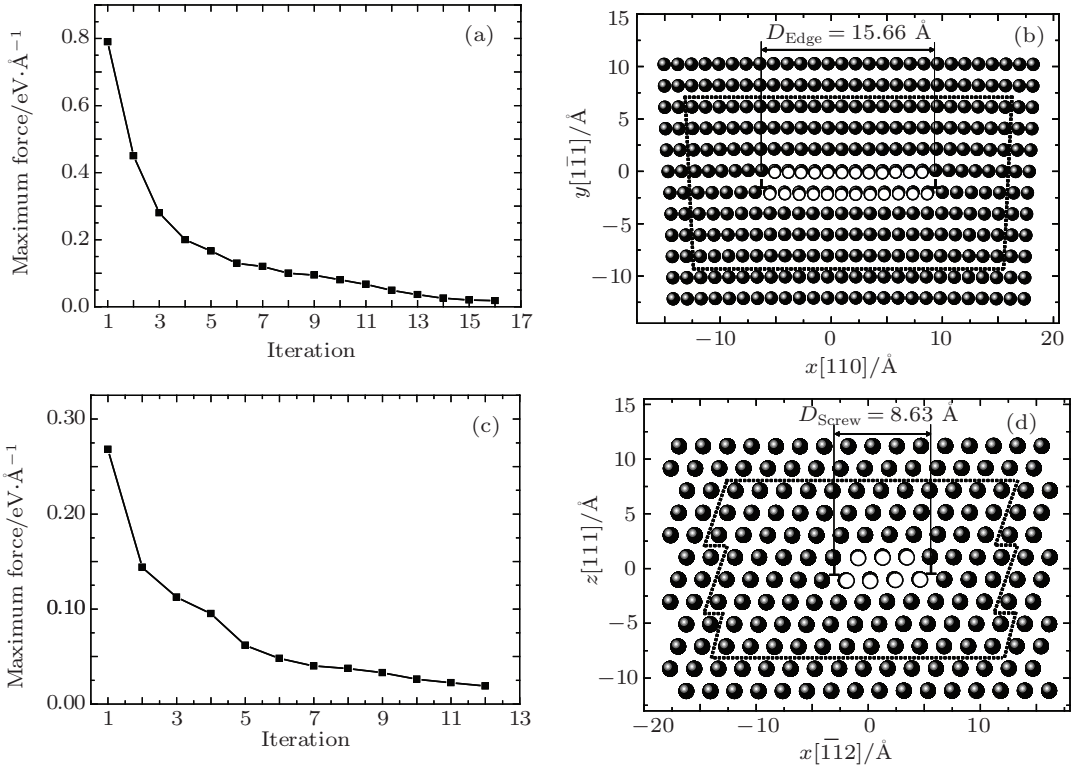


Fig. 4. Computational results for the edge and screw dislocations in Ni. (a) The maximum force on the coupling-region Ni atoms before MD relaxation in each iteration for an edge dislocation. (b) The core structure of the dissociated edge dislocation in Ni. (c) The maximum force on the coupling-region Ni atoms before MD relaxation in each iteration for a screw dislocation. (d) The core structure of the dissociated screw dislocation in Ni.

Table 2. The partial splitting distances for $a/2\langle 110\rangle$ edge and screw dislocations in Ni.

Method	Edge/Å	Screw/Å
Present work	15.66	8.63
EAM	14.9[a], 24.9[b]	7.4[a], 14.5[c], 25[d]
Experiment	18∼34[e]	–

[a]Ref. [6], [b]Ref. [32], [c]Ref. [33], [34], [d]Ref. [34], [e]Ref. [31]

Most available calculated results of dislocation core structure in Ni are given by MD simulations using EAM potentials as listed in Table 2.[6,32–34] The separation distances of partial dislocations predicted by MD are scattered because the results largely depend on the values of stacking fault energy produced by EAM potentials. The EAM potential used in the work of Szelestey *et al.*[6] produces a higher stacking fault energy $\gamma = 176$ mJ/m^2 than the experimental data[31] of 120 mJ/m^2∼130 mJ/m^2, which gives small splitting distances. The EAM potentials used in the work of Wen *et al.*[32,33] and Qi *et al.*[34] produce lower stacking fault energies $\gamma = 89$ mJ/m^2 and 40 mJ/m^2 respectively which give large splitting distances. In our previous work,[35] the stacking fault energy of pure Ni was calculated by DFT to be 125.25 mJ/m^2, which is in excellent agreement with the experimental result. This shows the necessity of treating the dislocation core by quantum mechanics.

4. Conclusions

Based on the positional continuity of atoms, we employed an iterative procedure to realize the QM/MM multiscale simulation. The applications of our method to Al and Ni systems confirmed the effectiveness of this approach in FCC metals. Compared to the earlier methods of QCDFT and FP-GFBC, the present method treats the coupling of long-range strain to the local displacements of the dislocation core in a simpler way with the same accuracy. The atomic core structure obtained by our QM/MM simulation can serve as the starting structure for studying the interaction between impurity and dislocation and the effects of alloying elements on the mechanical property of alloys.

Acknowledgements

The authors wish to thank Dr. Du Jun-Ping and Dr. Sun Min for helpful discussions.

References

[1] Schoeck G, Kohlhammer S and Fahnle M 1999 *Phil. Mag. Lett.* **79** 849
[2] Schoeck G 2001 *Philos. Mag.* A **81** 1161
[3] Lu G, Kioussis N, Bulatov V V and Kaxiras E 2000 *Phys. Rev.* B **62** 3099
[4] Lu G, Kioussis N, Bulatov V V and Kaxiras E 2001 *Mater. Sci. Eng.* A **309** 142
[5] Mryasov O N, Gornostyrev Y N, van Schilfgaarde M and Freeman A J 2002 *Acta Mater.* **50** 4545

[6] Szelestey P, Patriarca M and Kaski K 2003 *Modelling Simul. Mater. Sci. Eng.* **11** 883
[7] Yan J A, Wang C Y and Wang S Y 2004 *Phys. Rev.* B **70** 174105
[8] Wang C and Wang C Y 2009 *Chin. Phys.* B **18** 3928
[9] Vitek V 1968 *Philos. Mag.* **18** 773
[10] Vitek V 1974 *Cryst. Lattice Defects* **5** 1
[11] Choly N, Lu G, E W and Kaxiras E 2005 *Phys. Rev.* B **71** 094101
[12] Lu G, Tadmor E B and Kaxiras E 2006 *Phys. Rev.* B **73** 024108
[13] Liu Y, Lu G, Chen Z Z and Kioussis N 2007 *Modelling Simul. Mater. Sci. Eng.* **15** 275
[14] Zhang X and Lu G 2010 *Phys. Rev.* B **82** 012101
[15] Zhang X, Peng Q and Lu G 2010 *Phys. Rev.* B **82** 134120
[16] Woodward C and Rao S 2002 *Phys. Rev. Lett.* **88** 216402
[17] Woodward C and Rao S 2004 *Philos. Mag.* **84** 401
[18] Cawkwell M J, Nguyen-Manh D, Woodward C, Pettifor D G and Vitek V 2005 *Science* **309** 1059
[19] Woodward C, Trinkle D R, Hector L G Jr and Olmsted D L 2008 *Phys. Rev. Lett.* **100** 045507
[20] Leyson G P M, Curtin W A, Hector L G Jr and Woodward C 2010 *Nat. Mater.* **9** 750
[21] Kresse G and Hafner J 1993 *Phys. Rev.* B **47** 558
[22] Kresse G and Furthmuller J 1996 *Phys. Rev.* B **54** 11169
[23] Blochl P E 1994 *Phys. Rev.* B **50** 17953
[24] Kresse G and Joubert D 1999 *Phys. Rev.* B **59** 1758
[25] Perdew J P, Burke K and Ernzerhof M 1996 *Phys. Rev. Lett.* **77** 3865
[26] Monkhorst H J and Pack J D 1976 *Phys. Rev.* B **13** 5188
[27] Mishin Y, Farkas D, Mehl M J and Papaconstantopoulos D A 1999 *Phys. Rev.* B **59** 3393
[28] Honeycutt J D and Andersen H C 1987 *J. Phys. Chem.* **91** 4950
[29] Stukowski A 2010 *Modelling Simul. Mater. Sci. Eng.* **18** 015012
[30] Höllerbauer W and Karnthaler H P 1981 *Beitr. Elektronenmikroskop. Direktabb. Oberfl.* **14** 361
[31] Carter C B and Holmes S M 1977 *Philos. Mag.* **35** 1161
[32] Wen M, Fukuyama S and Yokogawa K 2005 *Scripta Mater.* **52** 959
[33] Wen M, Ngan A H W, Fukuyama S and Yokogawa K 2005 *Philos. Mag.* **85** 1917
[34] Qi Y, Strachan A, Cagin T and Goddard III W A 2001 *Mater. Sci. Eng.* A **309–310** 156
[35] Yu X X and Wang C Y 2009 *Acta Mater.* **57** 5914